Journal of Macromolecular Science, Part A
Publication details, including instructions for authors and subscription information:
http://www.informaworld.com/smpp/title~content=t713597274

Preparation and Characterization of Thermosensitive Nanoparticles for Targeted Drug Delivery

Jun Li[a]; Bochu Wang[a]; Yazhou Wang[a]; Peng Liu[a]; Weili Qiao[a]
[a] College of Bioengineering, Chongqing University, Chongqing, P.R.China

To cite this Article Li, Jun , Wang, Bochu , Wang, Yazhou , Liu, Peng and Qiao, Weili(2008) 'Preparation and Characterization of Thermosensitive Nanoparticles for Targeted Drug Delivery', Journal of Macromolecular Science, Part A, 45: 10, 833 — 838
To link to this Article: DOI: 10.1080/10601320802300685
URL: http://dx.doi.org/10.1080/10601320802300685

Journal of Macromolecular Science®, Part A: Pure and Applied Chemistry (2008) **45**, 833–838

ISSN: 1060-1325 print / 1520-5738 online
DOI: 10.1080/10601320802300685

Taylor & Francis
Taylor & Francis Group

Preparation and Characterization of Thermosensitive Nanoparticles for Targeted Drug Delivery

JUN LI, BOCHU WANG, YAZHOU WANG, PENG LIU and WEILI QIAO

College of Bioengineering, Chongqing University, Chongqing 400030, P.R.China

Received March 2008 and accepted April 2008

In this study, we have reported novel thermosensitive nanoparticles formulated by an emulsion-solvent evaporation technique using acetaminophen (AAP) as a model drug. The high entrapment efficiency of nanoparticles was 68.56%, particle size about 240.6 nm and zeta potential −27 mV. Furthermore, the drug release was also investigated both at 37°C and 42°C, respectively. The goal of our study was to obtain a targeted drug delivery system, exploiting the temperature-sensitive behavior. In contrary to normal temperature (37°C), the release rate of AAP was found to noticeably increase at high temperature (42°C) with a larger cumulative amount of drug released. In this way, it would lead to production of nanoparticles having a high thermosensitive behavior on drug release. Thus, this new strategy has the potential to control drug release at the diseased site for targeted drug delivery system (TDDS) with positive temperature-controlled.

Keywords: Drug delivery, phase transition, nanoparticles, thermosensitive, targeted

1. Introduction

Today, the concept of drug delivery is not limited to prolonging the duration of drug release; instead, it implies effective strategies for achieving therapeutic levels of drug at the diseased site without damaging healthy organs and tissues. Over the past decade, drug carrier systems have been developed that can retain drugs, evade the body's defenses, and target the diseased site. However, the ability to control release rate would be extremely advantageous and may prove to be an essential step in providing effective levels of drug in the targeted site. The biggest challenge, therefore, now facing drug delivery (for nanoparticles and other carriers) is to produce release of the encapsulated drug only at the diseased site and at controllable rates. Several strategies for controlling the drug release which can respond to different environmental conditions (temperature, pH, light, ionic strength, magnetic field, electric field, ultrasound, etc.) (1–7) have been developed. Among of them, one promising approach is to use temperature-sensitive nanoparticles to achieve this type of effect, and ground-breaking efforts have paved the way for many additional studies in recent years (8–11). Previous studies showed that the polymer properties, drug characterizations, particle size, and route of administration in a targeted drug delivery determine a given drug access to the target site (12–14).

Thermosensitive hydrogels have attracted increasing attention in the field of controlled drug release, to meet the need for prolonged and better control of drug administration (15–17). With these polymers, it is possible to administer the formulation as a solution, which undergoes a temperature-induced reversible phase transition upon heating or cooling of the aqueous solution. Typical thermosensitive hydrogels are poly(N-isopropylacrylamide) (PNIPAAm) and poly(ethylene oxide)-poly(propylene oxide)-poly(ethylene oxide) (PEO-PPO-PEO) triblocks. Use of these thermosensitive hydrogels would not only provide a sustained release formulation but also enhance the stability of drugs. Unfortunately, these polymers have drawbacks such as non-biocompatibility, toxic side effect, poor mechanical properties, limited stability and short residence times, which render these systems clearly unsuitable for drug delivery system. In recent years, many researchers have reported studies on new injectable and biodegradable polymers possessing reversible gelation properties in the drug delivery system. Poly(dl-lactide-co-glycolide)-polyethylene glycol-poly(dl-lactide-co-glycolide) (PLGA-PEG-PLGA) is a biocompatible, biodegradable and thermosensitive hydrogel (18), and it has been widely studied for biomedical and pharmaceutical applications (19–21). However, a great many researches were focused on improving controlled-release properties of this thermosensitive hydrogel carriers based on the sol-gel transition, whereas the research for targeted drug delivery has been rarely reported until now.

Address correspondence to Bochu Wang, College of Bioengineering, Chongqing University, Chongqing, 400030, P.R.China. Tel: 86-23-65112840; Fax: 86-23-65112877; E-mail: wangbc2000@126.com

Indeed, thermosensitive polymers have potential applications in targeted drug delivery, especially in delivering drug to tumor sites (22, 23).

Therefore, the purpose of the present study was to develop novel thermosensitive nanoparticles for targeted drug delivery, and, the two main contributions of this paper were (i) to synthesize a biodegradable thermosensitive hydrogel with the effective property of phase transition temperature; (ii) to furnish one approach potentially for targeted drug delivery with an on-off switch response to temperature change.

2. Experimental

2.1. *Materials*

Polyethylene glycol (PEG 1000, PEG1500) were purchased from Chongqing Chemical Reagent Co. in China. D,L-Lactide and Glycolide were purchased from Shandong Biomedicine Co. Stannous 2-ethylhexanoate (Stannous Octoate) was purchased from Sigma Chemical Co., St. Louis, MO, USA. Polyvinyl alcohol (Poval 205S PVA) was purchased from Kuraray Co. Ltd, Japan. Acetaminophen (AAP) was supplied by Anqiu Lu'an Pharmaceutical Co. Ltd, China. All other chemicals were of analytical grade.

2.2. *Ring-opening polymerization*

The PLGA-PEG-PLGA hydrogel was prepared according to a previously published method (24), but with several modifications. Briefly, under nitrogen atmosphere, 20 g polyethylene glycol (PEG1000, PEG1500) were dried in a three-necked flask under vacuum and stirred at 160°C for 2 h. D,L-lactide (37.82 g) and glycolide (11.6 g) were added and stirred for 30 min. Then, stannous 2-ethylhexanoate was added and the reaction mixtures were kept in an oil bath at 150°C for 8 h. The product was dissolved in ice water (5°C-8°C). After it was completely dissolved, the copolymer solution was heated to 80°C to precipitate the copolymer and to remove the water-soluble low-molecular weight copolymer and unreacted monomers. The supernatant was decanted to obtain the precipitated copolymer. The process was repeated three times to purify the copolymer. Finally, the polymer was freeze-dried for complete removal of the residual water and was storied at −20°C until further use.

2.3. *NMR spectrometry*

An NMR spectrometer (Bruker, 500 MHz) was used for ^{1}H-NMR spectra of PLGA-PEG-PLGA triblock copolymer at room temperature. The solvent used was deuterated chloroform ($CDCl_3$). TMS signal was taken as the zero chemical shift.

2.4. *Phase transition*

The phase transition was measured by a test tube inverting method with temperature increments of 1°C per each step (25). The PLGA–PEG–PLGA triblock copolymers having concentrations of 10, 15, 20, 25 wt%, respectively, were dissolved into distilled water in vials. After equilibration at 4°C for 12 h, the vials containing samples were immersed in a water bath at a constant designated temperature, ranging from 15°C to 55°C. Before being measured at each constant temperature, the sample was kept for 20 min to allow the establishment of equilibrium. The gel state was determined by inverting the vial horizontally when no fluidity in 1 min was visually observed.

2.5. *Preparation of thermosensitive nanoparticles*

PLGA-PEG-PLGA NPs encapsulating AAP were prepared using an emulsion-solvent evaporation technique. Briefly, acetaminophen was dissolved in acetone, and the polymer was added into the solution. NPs were formed by adding the drug–polymer solution to a stirring PVA solution. The resulting NP suspension was allowed to stir uncovered for 6 h at room temperature. NPs were purified by centrifugation at 19000 rpm for 30 min (JA-20 Beckman Coulter Avanti® J-E centrifuge). The PLGA-PEG-PLGA-NPs were resuspended, and washed with water three times. Finally, the NPs were collected by after being freeze-dried for 48 h.

2.6. *Particles size distribution and surface charge*

Particle size and size distribution was determined by photon correlation spectroscopy (PCS) under a fixed angle of 90°. The PCS analysis yielded the mean diameter of the particles (Z-average) and the polydispersity index (PI) as a measure of the width of the particle size distribution. The sample was subjected to particle size analysis in the Zetasizer Nano ZS 90 (Malvern Instruments Ltd., Malvern UK). The mean hydrodynamic diameter was determined by cumulative analysis. The surface charge of the hydrogel particle was determined by measurements of the zeta potential carried out with the same instrument.

2.7. *Determination of drug loading*

Drug encapsulation efficiency was determined by measuring the amount of free drug remaining in the supernatant solution, not in the nanoparticles after collection by being freeze-dried. The supernatant was analyzed for AAP content by measuring the optical density of wavelength of 243 nm (UV752S, Shanghai, China). Encapsulation efficiency (EE, %) was calculated by the following formula:

$$\text{Encapsulation efficiency (\%)} = \frac{\text{drug in nanoparticle}}{\text{drug added}},$$

Where the drug in nanoparticle = the drug added − the free drug remained in the supernatant.

2.8. *In vitro release study*

Twenty milligrams of nanoparticles was dispersed in a 5 ml PBS buffer. The solution was then filled into a dialysis tubing and incubated in 50 ml PBS with gentle shaking (200 r/min) at 37°C and 42°C, respectively. At scheduled time intervals, 10 ml of the dissolution medium was collected, and the remaining dissolution medium was immediately replenished with pure PBS to maintain the original volume. The concentration of released AAP was monitored at 243 nm using the UV spectrophotometer. Each experiment was performed in triplicate and the results were reported as mean ± standard deviation.

3. Results and discussion

3.1. *H-NMR analysis*

The PLGA-PEG-PLGA triblock copolymer was synthesized by ring-opening polymerization of D,L-lactide and glycolide with polyethylene glycol (PEG) in the presence of stannous octoate. In order to gain insight into its chemical structure, the PLGA–PEG–PLGA triblock copolymer was analyzed using ^{1}H-NMR spectrometry. A typical spectrum of the polymer is presented in Figure 1. The signals pertaining to PLGA–PEG–PLGA are found in a) $\delta = 5.15$ ppm (CH of LA; b)1.52 ppm (CH_3 of LA; c) 4.76 ppm (CH_2 of GA, d); 3.58 ppm (CH_2 of ethylene glycol).

This spectrum was similar to the reported spectrum and all the signals were assigned on the spectrum (26). The bands at 5.15 and 1.52 ppm were assigned to the methine and methyl protons of PLGA blocks, respectively, while the bands at 3.58 ppm are characteristic of main chain methylene groups in the PEG blocks. The multiplet at 4.76 ppm corresponds to CH_2 protons of PLGA end units together with CH_2-linking ethylene glycol of PEG blocks. These features agree well with the formation of triblock copolymers. The hydrophobicity of the copolymer reinforces by increasing the molar ratio of D, L-lactide/glycolide in the PLGA segment because D, L-lactide moiety is more hydrophobic than glycolide. The amphiphilicity of PLGA-PEG-PLGA copolymer mainly depends on the D, L-lactide/glycolide ratio and PEG content which have much influence on the phase transition temperature.

3.2. *Thermosensitive properties of PLGA–PEG–PLGA triblock copolymer*

In this paper, the sol (flow) and gel (non-flow) are defined by the flow characteristics when a solution contained in the vial is inverted at a given temperature. This definition is also well correlated with the falling ball method and dynamic mechanical analysis (27). The aqueous solution of PLGA-PEG-PLGA exhibits four phase states, as following: The solution flows freely below the physiological temperature, and becomes a gel at physiological temperature, then flows freely again as temperature increases, ultimately undergoes insoluble precipitate.

In this study, temperature from sol to gel is defined as lower transition temperature, and temperature from gel to

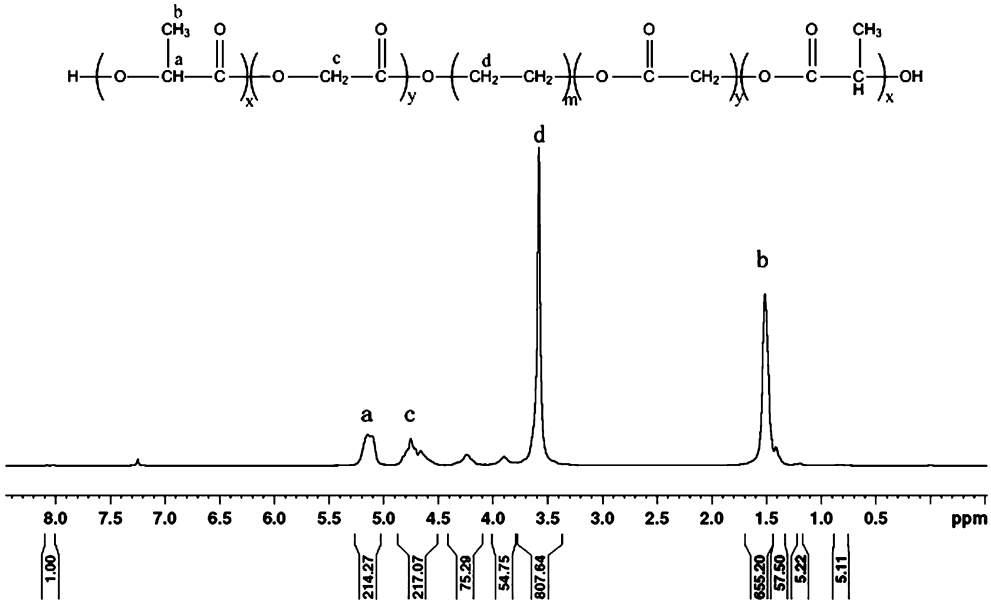

Fig. 1. The typical ^{1}H-NMR spectra of PLGA–PEG–PLGA triblock copolymer (a) CH of LA, (b) CH_3 of LA, (c) CH_2 of GA, (d) CH_2 of ethylene glycol.

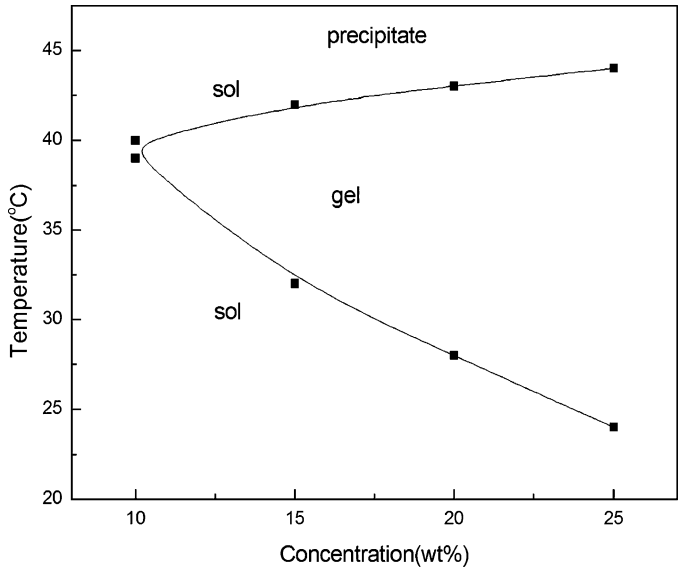

Fig. 2. Effect of polymer concentration on transition temperature of aqueous solutions of PLGA–PEG–PLGA.

sol is defined as upper transition temperature. From 15°C to 55°C, its aqueous solutions presented four physical states: sol, gel, sol and precipitate. The phase chart of this triblock copolymer in water demonstrates the transition temperature curve, which is presented in Figure 2. When the copolymer concentration increased from 10% to 25%, sol-gel transition temperature decreased from 39°C to 24°C and gel–sol transition temperature increased from 40°C to 44°C. Thus, we can modify polymer concentration to meet specific requirements in drug delivery systems, especially for targeted drug delivery system, based on the gel–sol transition when temperature increased from the normal temperature (37°C) to hyperthermic temperatures (40°C–44°C).

The phase transition of the PLGA-PEG-PLGA triblock copolymer aqueous solution was similar to the reported result (28)except for the presence of the gel-sol transition temperature about 40°C to 44°C, when the concentration of the polymer increased from 10 to 25 wt%. In the case of 10 wt% aqueous solution of PLGA-PEG-PLGA, there was clear flow at low temperature, and the sol state was maintained until 39°C. Moreover, a further temperature increase made the gel state flow in the vial tilting test. Micellar aggregate formation was suggested for the sol to gel transition (lower transition), whereas an increase in the PLGA molecular motion and disruption of micellar structure was proposed for the gel-sol transition (upper transition) for the PLGA-PEG-PLGA triblock copolymer aqueous solution(29). At lower temperatures, hydrogen bonding between hydrophilic PEG segments of the copolymer chain and water molecules dominated in the aqueous solution, resulting in their dissolution in water(30). As the temperature increased, the hydrogen bonding became weaker, while hydrophobic forces among the hydrophobic PLGA segments strengthened leading to sol-gel transition. With a further increase in temperature, the gel underwent a gel-sol transition. At last, the PEG was partially dehydrated with a macroscopic phase separation between water and polymers.

3.3. *Physicochemical characterization of thermosensitive nanoparticles*

The thermosensitive PLGA-PEG-PLGA-NPs suspension was obtained using the emulsion-solvent evaporation process. Parameters controlling formation of the NPs were systematically varied in this study. Generally, the starting formulation was as follows: PLGA-PEG-PLGA (10 mg/ml) and acetaminophen (0.1 mg/ml) were dissolved in acetone. The mixture was added dropwise to a 1 volume of stirring PVA solution. The effects of PVA concentrations and polymer concentrations were assayed on the overall size of the NPs. PVA concentrations was varied from 1 to 5 wt%, and a range of polymer concentrations in the organic phase from 5 mg/ml to 20 mg/ml was used for formation of NPs. The encapsulation efficiency of NPs changed between 23.87% and 68.56%, depending on different process parameters. The highest AAP encapsulation efficiency was obtained with the formulation prepared by 10 mg/ml PLGA-PEG-PLGA concentration and 1% PVA concentration.

The average size of NPs with various process parameters changed between 152.4 nm and 361.5 nm, and, when polymer concentrations were varied during NP formulation at a fixed PVA concentration, we observed a trend of increasing NP sizes with increasing polymer concentration. For example, NP sizes increased from 183.4 nm to 302.8 nm in 1 wt% PVA concentration as the polymer concentration increased from 5 to 20 mg/ml. In addition, similar trends were observed in various PVA concentrations (2.5 and 5 wt%). Most interestingly, the data in terms of changes in nanoparticles size showed linear agreement between size and polymer concentration in various PVA concentrations. The R^2 values for the plot of mean NP size and polymer concentration (Figure 3) were 0.98626, 0.99877, and 0.99635 for 1, 2.5, and 5 wt% PVA concentration, respectively. In a previous study, the linear correlation between volumetric size of PLGA–PEG nanoparticles and polymer concentration was also reported (31). In our polymeric drug delivery system, using the linear correlation of the NP size and polymer concentration can allow for formulation of NP with predefined, desirable sizes. Figure 3 also displayed the effect of PVA concentrations on the size of nanoparticles. It was shown that the smallest particles were found in 2.5% PVA, while both higher and lower PVA concentrations (5 wt% and 1 wt %) led to larger particles. In the emulsion-solvent evaporation technique, PVA as a stabilizer to nanoparticles emulsion, was attached to the surface of nanoparticles, to avoid gathering among the particles (32). Therefore, the particle size could diminish with the

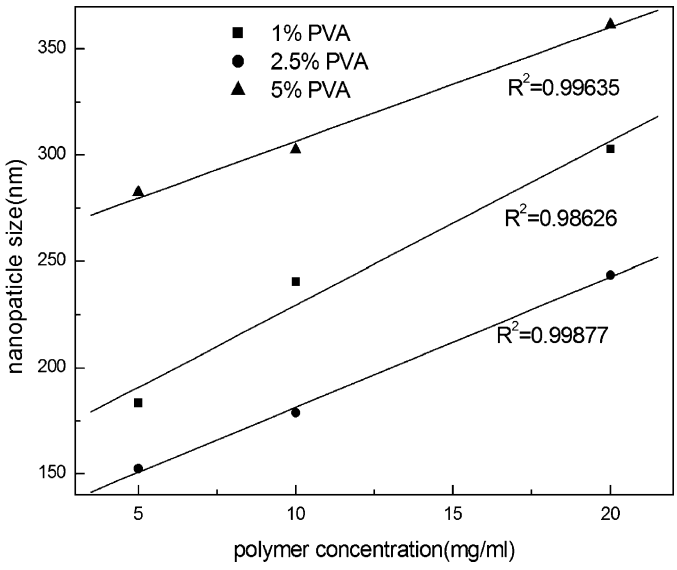

Fig. 3. Plot of the nanoparticles size and polymer concentration in various PVA concentrations.

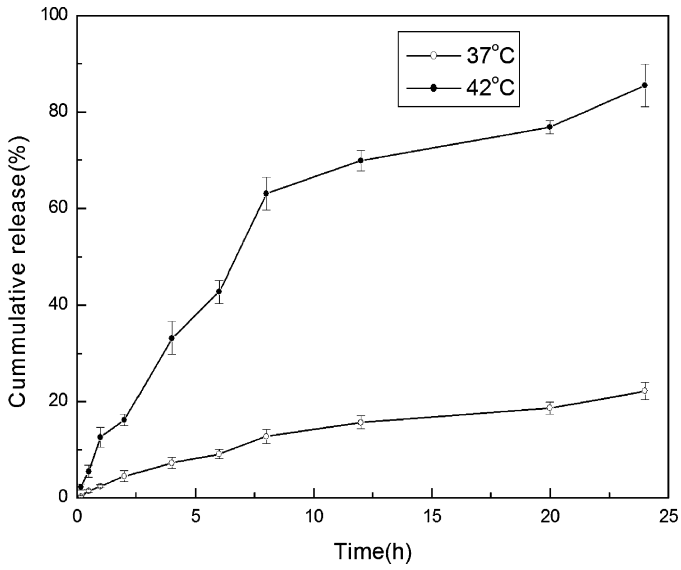

Fig. 4. Release of AAP from thermosensitive nanoparticles at 37°C and 42°C.

PVA concentration increasing from 1 to 2.5 wt%. But the higher PVA concentration (5 wt%) may induce the viscous dispersed phase, which was not favorable to the diffusion of the oil phase(33).Moreover, more PVA molecules attach to the nanoparticles may also lead to produce larger particles.

3.4. *In vitro release study*

Release of AAP from PLGA-PEG-PLGA nanoparticles prepared with the parameters of polymer concentration (10 mg/ml) and PVA concentration (1 wt%) was investigated *in vitro*. Figure 4 shows the cumulative drug release in PBS at two temperatures (37and 42°C). This figure clearly shows that the drug is released faster in a hot environment (42°C) than in a physiological environment (37°C). As can be seen, the release of AAP at 37°C is slow and sustained, with only about 7% of the total drug content being released within the first 4 h. Drug release at 42°C is, however, much faster, close to 33% within the first 4 h, and nearly 63% by the first 8 h. The drug release has a noticeable increase at 42°C, which may be attributed to the phase transition of PLGA-PEG-PLGA. As shown in Figure 2, the aqueous solution of the hydrogel becomes a gel at 37°C, and flows freely in a high temperature (42°C). So, these thermosensitive nanoparticles can undergo reversible structural transitions from a closed state to an open state, giving on-off switches in respond to temperature for modulating drug delivery. The drug release curve (Figure 4) and the phase transition curve (Figure 2) support that our TDDS design is effective in giving a positive drug controlled release, i.e., drug release rate is accelerated at an increased temperature above the normal temperature in the body.

On the other hand, evidence that the drug release responds to temperature is that the PLGA-PEG-PLGA nanoparticles exhibited a size change with increasing temperature. The average diameter was decreased from 240.6 nm to 192.6 nm with increasing temperature from 25°C to 44°C, as shown in Figure 5. The nanoparticles size had a slight decrease from 25°C to 40°C, however, a sharp decrease at 42°C. This would lead to production of nanoparticles having a high thermosensitive behavior on drug release. At the lower temperature, a PEG segment expanded into the water phase, owing to the

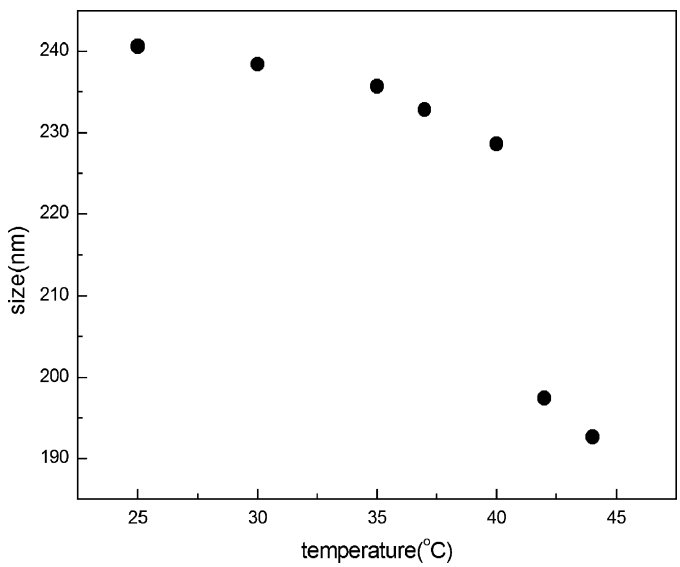

Fig. 5. Nanoparticles size change with temperature ranging from 25°C to 44°C.

formation of hydrogen bond between PEG and water molecules. Meanwhile, AAP was fixed in the PLGA segment by hydrophobic attractions. Nanoparticles were in a stable state in the disperse phase, attribution to the equilibration of the PEG segment and hydrophobic core. However, when the temperature increased to 42°C, the disrupted hydrogen bonds and broken equilibration would lead to the shrinking particles, and the drug of AAP was expelled from the nanoparticles quickly. Additionally, the change in surface zeta potential values provides more evidence of an increase in charge density when the temperature increases. This may be caused by the drug release of highly charged nanoparticles with increasing temperature. The surface charge of the PLGA-PEG-PLGA nanoparticles greatly increases from −27 mV at 37°C to −40.02 mV at 42°C in our study.

Our *in vitro* studies show the advantages that the novel nanoparticles have a significant impact on drug release at 37°C and 42°C, respectively. In this way, the dominant challenge of our study is the control of the rate of drug release: Drug doses may fit within a specific window that the release rate on a diseased site has a significant increase in contrast to a healthy site by creating local hyperthermia owing to heat generation, and thereby offers the potential to control drug release at the diseased site.

4. Conclusions

In summary, using a emulsion-solvent evaporation technique, we have successfully synthesized PLGA-PEG-PLGA nanoparticles with AAP as a model drug. The resulting thermosensitive NPs retained the high temperature-sensitive capability. The temperature induced interior structural changes of the nanoparticles at 42°C led to accelerated AAP release in contrast to the normal temperature (37°C). In particular, the nanoparticles showing linear agreement between size and polymer concentration could offer a great size-controlled functionality. This thermosensitive drug system has not yet been optimized and we believe that accumulation of the thermosensitive carriers in high temperature at the diseased site can offer the possibility of further improving the efficiency of targeted delivery.

Acknowledgment

This work was supported by Chongqing University Postgraduates' Science and Innovation Fund (Project No. 200603Y1A0120155).

References

1. Vihola, H., Laukkanen, A., Hirvonen, J. and Tenhu, H. (2002) *Eur. J. Pharm. Sci*., 16, 69–74.
2. Siemoneit, U., Schmitt, C. and Alvarez-Lorenzo, C. (2006) *Int. J. Pharm.*, 312, 66–74.
3. Paasonen, L., Laaksonen, T., Johans, C., Yliperttula, M., Kontturi, K. and Urtti, A. (2007) *J. Controlled Release,* 122, 86–93.
4. Alvarez-Lorenzo, C., Gonzalez-Lopez, J., Fernandez-Tarrio, M., Sandez-Macho, I. and Concheiro, A. (2007) *Eur. J. Pharm. Biopharm.,* 66, 244–252.
5. Besheer, A., Wood, K.M., Peppas, N.A. and Mäder, K. (2006) *J. Controlled Release,* 111, 73–80.
6. Peng, Z.G., Hidajat, K. and Uddin. M.S. (2004) *Colloids Surf. B Biointerfaces*, 35, 169–174.
7. Sershen, S. and West, J. (2002) *Adv. Drug Deliv. Rev.,* 54, 1225–1235.
8. Choi, S.H., Lee, S.H. and Park, T.G. (2006) *Biomacromolecules,* 7, 1864–1870.
9. Zhu, M.Q., Wang, L.Q. and Exarhos, G.J. (2004) *J. Am. Chem. Soc.,* 126, 2656–2657.
10. Shamim, N., Hong, L., Hidajat, K. and Uddin, M.S. (2007) *Colloids Surf. B Biointerfaces*, 55, 51–58.
11. Stovera, T.C., Kim, Y.S., Lowe, T.L. and Kester, M. (2008) *Biomaterials,* 29, 359–369.
12. Kong, G., Braun, R.D. and Dewhirst, M.W. (2000) *Cancer Res.,* 60, 4440–4445.
13. Yamaoka, T., Makita, Y., Sasatani, H., Kim, S.I. and Kimura, Y. (2000) *J. Controlled Release,* 66, 187–197.
14. Jin, S. and Ye, K. (2007) *Biotechnol. Prog.,* 23, 32–41.
15. Ramanan, R.M.K., Chellamuthu, P., Tang, L. and Nguyen, K.T. (2006) *Biotechnol. Prog.*, 22, 118–125.
16. Couffin-Hoarau, A.C. and Leroux, J.C. (2004) *Biomacromolecules*, 5, 2082–2087.
17. Alvarez-Lorenzoa, C., Concheiroa, A. and Dubovik, A.S. (2005) *J. Controlled Release,* 102, 629–641.
18. Pratoomsoot, C., Tanioka, H. and Hori, K. (2008) *Biomaterials,* 29, 272–281.
19. Kwon, Y.M. and Kim, S.W. (2004) *Pharm. Res.*, 21, 339–343.
20. Moffatt, S. and Cristiano, R.J. (2006) *Int. J. Pharm.,* 321, 143–154.
21. Choi, S. and Kim, S.W. (2003) *Pharm. Res.,* 20, 2008–2010.
22. Rapoport, N. Prog. (2007) *Polym. Sci.,* 32, 962–990.
23. Choi, S.W. and Kim, J.H. (2007) *J. Controlled Release*, 122, 24–30.
24. Zenter, G.M., Rathi, R. and Shih, C. (2001) *J. Controlled Release,* 72, 203–215.
25. Jeong, B., Bae, Y.H. and Kim, S.W. (1999) *Macromolecules,* 32, 7064–7069.
26. Qiao, M.X., Chen, D.W. and Ma, X.C. (2005) *Int. J. Pharm.,* 294, 103–112.
27. Chung, Y.M., Simmons, K., Gutowska, A. and Jeong, B. (2002) *Biomacromolecules,* 3, 511–516.
28. Duvvuri, S., Janoria, K.G. and Mitra, A.K. (2005) *J. Controlled Release,* 108, 282–293.
29. Chen, S., Pieper, R., Webster, D.C. and Singh, J. (2005) *Int. J. Pharm.,* 288, 207–218.
30. Fujiwara, T., Mukose, T., Yamaoka, T., Yamane, H. and Sakurai, S. (2001) *Macromol. Biosci.*, 1, 204–208.
31. Chenga, J., Teplya, B.A., Sherifi, I. and Farokhzad, O.C. (2007) *Biomaterials,* 28, 869–876.
32. Kwon, H.Y., Lee, J.Y., Choi, S.W., Jang, Y. and Kim, J.H. (2001) *Colloids Surf., A: Physicochem. Eng. Aspects,* 182, 123–130.
33. Li, J.K., Wang, N. and Wu, X.S. (1998) *J. Controlled Release,* 56, 117–126.